Assembly Depletion and Equilibrium Cycle Core Verification of the Soluble-Boron-Free SMR PRATIC benchmark Using STREAM/RAST-K

Jihyeon Lee, Yeongseok Kang, Deokjung Lee*
Department of Nuclear Engineering, Ulsan National Institute of Science and Technology (UNIST), Ulsan, 44919, Republic of Korea
**Corresponding author: deokjung@unist.ac.kr*

Keywords : SMR, soluble-boron-free, PRATIC benchmark

1. Introduction

Small Modular Reactors (SMRs) are increasingly regarded as a flexible complement to large-scale nuclear power plants. The advantages of SMRs include standardized manufacturing, reduced capital cost, and siting flexibility. Among SMR concepts, Soluble-Boron-Free (SBF) designs have attracted particular interest. SBF operation simplifies the chemical and volume control system, reduces borated liquid waste, and eliminates boron dilution accidents. In SBF cores, reactivity is controlled by control rods and gadolinium-bearing burnable absorbers instead of soluble boron.

The PRATIC benchmark was developed by the French Atomic Energy and Alternative Energy Commission (CEA) to provide a common reference for evaluating neutronics methods for SBF SMR cores [1]. Reference solutions for the benchmark were generated using the APOLLO2.8-5/CRONOS2 code system with the JEFF-3.1.1 nuclear data library, and several research groups have investigated the benchmark using various deterministic and Monte Carlo codes [2-4].

In this work, the STREAM/RAST-K code system [5, 6] with the ENDF/B-VII.1 library is employed to analyze the PRATIC benchmark. The analysis spans from the assembly-level depletion characteristics of the five fuel assembly types to the core-level evaluation based on the equilibrium cycle search. Key core parameters such as core reactivity, cycle length, peaking factors, and axial offset, as well as the radial power and burnup distributions, are evaluated and compared against the CEA reference solutions.

2. Methodology

2.1 PRATIC Benchmark Description

PRATIC is a light water cooled SBF SMR benchmark with a thermal power of 350 MWth. The core consists of 57 fuel assemblies and operates at a system pressure of 155 bar. The active core region is surrounded by a heavy steel reflector to reduce neutron leakage and extend the cycle length. The active fuel height is 200 cm, approximately equal to the core diameter. The main design parameters of the core are listed in Table I.

Table I: Nominal operating conditions of PRATIC core

Data	Value
Nominal power (NP)	350 MWth
Specific power density	24.73 W/g
Number of fuel assemblies (FA)	57
FA pitch at 300℃	21.5313 cm
FA intergap at 300℃	0.04035 cm
Active height at 300℃	200.5613 cm
Primary system pressure	155 bar
Moderator inlet temp. (100% NP)	285℃
Moderator mass flow rate	2185.39 kg/s

Two distinct core configurations are defined in the benchmark to evaluate both initial and steady-state core characteristics. The startup core is loaded entirely with fresh fuel, utilizing five different assembly types where the enrichment is adjusted by core position to limit the initial excess reactivity. The equilibrium core is built from three of the five types and represents a converged 2-batch reload pattern. Fig. 1 presents the loading and refueling pattern of the equilibrium core.

Table II lists the specifications of the five assembly types. Each fuel assembly adopts a 17 by 17 lattice with 264 fuel rods, 24 guide tubes, and one instrumentation tube. Excess reactivity is suppressed by gadolinia burnable absorber (BA) rods, which contain 2 and 8 wt% Gd_2O_3 in a 2.5 wt% enriched UO_2 matrix regardless of the assembly enrichment. The Internal 2 and External 2 assemblies are used only in the startup core.

Table II: Fuel assembly specifications

FA Type	UO_2 wt%	Gd_2O_3 wt%	# of BA rods
Central	2.50	8	8
Internal 1	3.50	8	36
Internal 2	1.60	0	0
External 1	5.00	8	28
External 2	2.80	2 / 8	4 / 4

Consistent with the SBF concept, a control rod cluster is accommodated at every assembly position. Banks G1 to G3 are grey banks that combine 16 AIC

(Ag-In-Cd) rods with 8 stainless steel rods, whereas bank G4 is a black bank composed of 24 AIC rods. Shutdown banks with the same composition as the black bank occupy the remaining positions. Successive banks are inserted with a 50 % overlap to provide smooth reactivity control. Fig. 2 shows the arrangement of the control rod banks.

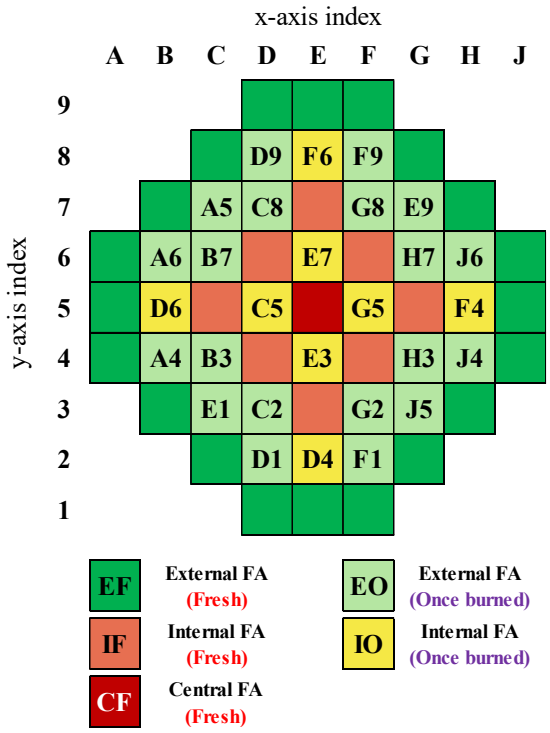


Fig. 1. Loading and refueling pattern of the PRATIC equilibrium core.

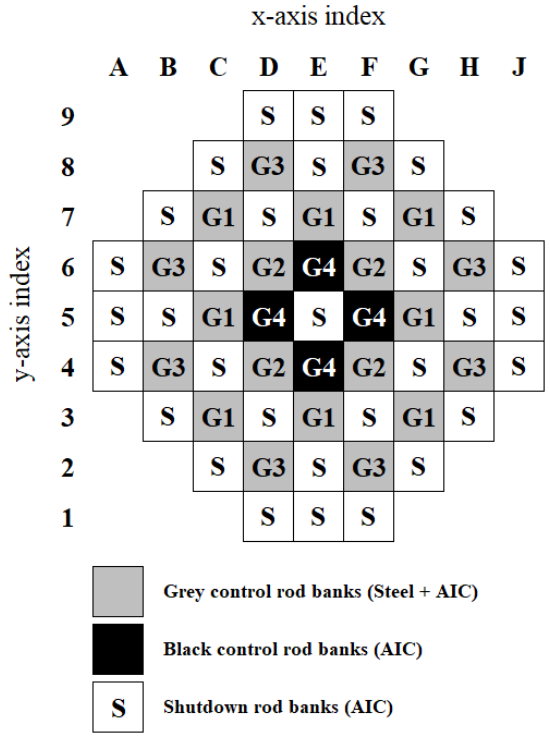


Fig. 2. Control bank arrangement of the PRATIC core.

2.2 Calculation Method

The analysis is performed with the STREAM/RAST-K code system. In the lattice calculation, STREAM solves the 2-D transport problem based on the Method of Characteristics (MOC). The resonance self-shielding effect is treated with the Pin-based Pointwise Energy Slowing Down Method (PSM) [5]. The homogenized few-group constants and assembly discontinuity factors (ADFs) generated for each assembly type are then passed to RAST-K. The 3-D nodal diffusion code RAST-K performs the fuel depletion, thermal-hydraulic feedback, and the critical rod search. The calculations in this work employ the ENDF/B-VII.1 library. The CEA benchmark provides assembly solutions for both JEFF-3.1.1 and ENDF/B-VII.1, and the ENDF/B-VII.1 solution is used for the assembly-level comparison so that the nuclear data effect is excluded. The core-level reference solution is available only with JEFF-3.1.1.

2-D assembly depletion calculations are performed for the five assembly types under reflective boundary conditions. For the equilibrium core, the cycle search is carried out through successive 2-batch reloading and depletion calculations. The cycle is considered converged when the difference in the end-of-cycle (EOC) core average burnup between two consecutive cycles falls below 15 MWd/MTU. The EOC is defined as the burnup at which the core reactivity in the All-Rods-Out (ARO) configuration reaches 100 pcm.

3. Results and Discussion

3.1 Assembly-Level Depletion Analysis

Fig. 3 compares the k_∞ evolution of the five assembly types calculated by STREAM with the reference solutions. The k_∞ behavior is governed by the competition between fissile depletion and gadolinium burnout, and the burnup at which the reactivity peak occurs depends on the gadolinium loading and the fuel enrichment.

The benchmark provides assembly solutions for both JEFF-3.1.1 and ENDF/B-VII.1. The nuclear data effect can therefore be quantified independently of the calculation scheme. Table III compares two quantities. The library effect is the difference between the two APOLLO2 solutions. The scheme effect is the difference between STREAM and APOLLO2 obtained with the same library. The library effect reaches an RMS of 275 pcm and a maximum of 695 pcm for the Internal 2 type. The value exceeds the corresponding scheme RMS of 147 pcm. A comparable magnitude is observed for the Central and External 2 types. The scheme effect becomes dominant only for the Internal 1 and External 1 types with large gadolinia loading. The nuclear data effect is therefore not negligible at the assembly level. The comparison presented below employs ENDF/B-VII.1 for both codes so that the deviation represents the difference between the calculation schemes alone.

The two codes agree well over the entire depletion range, and the reactivity difference remains within about 600 pcm for all assembly types. The scheme RMS listed in Table III increases with the number of BA rods, which indicates that the gadolinium treatment is the main source of the deviation. The gadolinia-free Internal 2 type shows the smallest difference. The Internal 1 and External 1 types with 36 and 28 BA rods show the largest discrepancies.

The reactivity difference evolves in three distinct stages, and the dominant source changes with burnup. At the beginning of depletion, STREAM predicts a higher reactivity, and the deviation grows with the gadolinium loading, up to 450 pcm for the Internal 1 assembly. During the gadolinium depletion phase, the difference turns negative, which indicates a small shift in the predicted burnout timing between the two codes. After the gadolinium is fully consumed, the difference increases again with burnup and reaches 300 to 550 pcm at 60 GWd/MTU. Both solutions are based on the same library. The growth therefore reflects the difference in the depletion treatment rather than the nuclear data. However, the impact of these deviations on the core calculation is limited, because the maximum discharge burnup of the equilibrium core is well below 60 GWd/MTU.

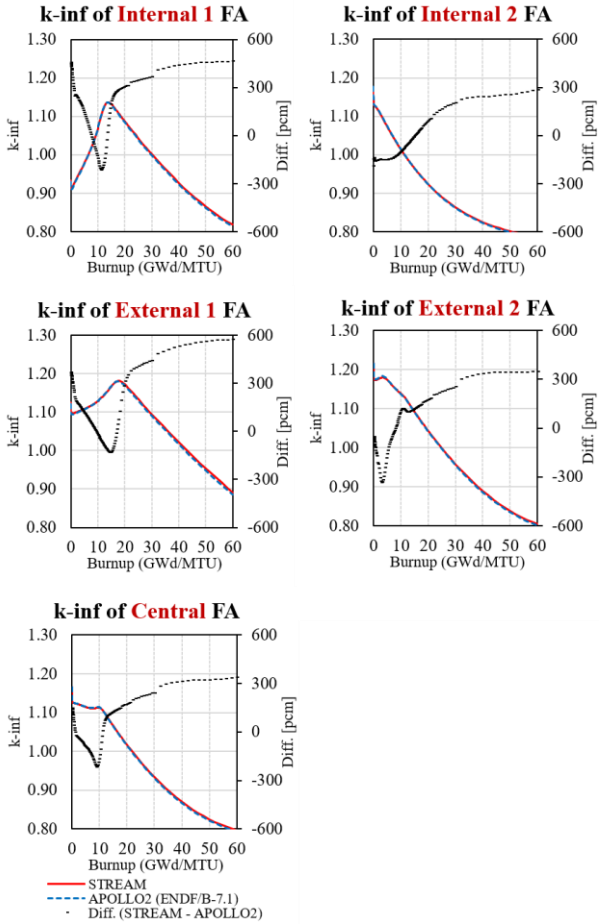


Fig. 3. Comparison of k_∞ between STREAM and APOLLO2 and reactivity difference of the five fuel assembly types.

Table III: Library effect and scheme effect on the assembly k_∞ (pcm)

FA Type	Lib. RMS	Lib. max	Sch. RMS	Sch. max
Central	214	563	171	335
Internal 1	128	334	283	462
Internal 2	275	695	147	-286
External 1	230	431	280	573
External 2	268	531	192	346

Library effect = APOLLO2 (ENDF/B-VII.1) - APOLLO2 (JEFF-3.1.1);
Scheme effect = STREAM - APOLLO2

3.2 Core-Level Analysis of the Equilibrium Cycle

The cycle search converged to an equilibrium cycle length of 17.550 GWd/MTU, which is 2.35% longer than the reference value of 17.148 GWd/MTU. Unlike the assembly comparison, the core-level reference is available only with JEFF-3.1.1, so the deviation includes both the library and the scheme contributions.

Fig. 4 shows the effective multiplication factor (k_{eff}) of the core in the ARO and All-Rods-In (ARI) configurations over the cycle. Both configurations are evaluated with the thermal-hydraulic conditions of the corresponding critical rodded states. RAST-K predicts a higher ARO k_{eff} than the reference over the cycle. The largest deviation of about 380 pcm appears at the beginning-of-cycle (BOC), and the value settles between 170 and 230 pcm over the remaining depletion range. The higher excess reactivity is directly reflected in the control rod behavior. Only the G1 and G2 banks are inserted during the cycle, and the G3 and G4 banks remain withdrawn. RAST-K inserts the G1 bank over the entire active height at BOC, which is about 26 cm deeper than the CRONOS2 result. The G2 bank follows with the same 50% overlap and shows a similar difference. The gap falls below 10 cm within 1 GWd/MTU and stays near 8 cm through the middle of the cycle. The gap widens again to about 15 cm near 13 GWd/MTU, where the G2 bank is fully withdrawn. In the ARI configuration, the deviation changes sign near 7.5 GWd/MTU, decreasing from about 520 pcm at BOC to about -670 pcm at EOC. The opposite trends in the two configurations indicate a difference in the total control rod worth between the two code systems, which becomes more pronounced toward the EOC. The maximum ARI k_{eff} is 0.809 at BOC, which confirms that the core remains subcritical with a sufficient margin throughout the cycle.

RAST-K predicts lower peaking factors than the reference over most of the cycle. The maximum deviation of Max-F_{xy} is about -2.7% near 10 GWd/MTU, and F_q deviates by up to about -11% at EOC. The G2 bank occupies four positions next to the core center, and the G1 bank forms a ring in the intermediate region. The deeper insertion therefore suppresses the power in the inner region and flattens the radial profile during the early and middle part of the cycle. The axial offset (AO) follows the reference trend

and stays negative until 12.5 GWd/MTU. The AO then rises sharply toward EOC. The rise occurs in the burnup range where the G2 bank is withdrawn and the G1 bank alone controls the core. The AO deviation remains within about 4% at BOC, but reaches about -11% after 15 GWd/MTU, which indicates that the upward power shift caused by the rod withdrawal is milder in RAST-K. The same behavior explains the F_q deviation at EOC, since a less pronounced axial peak lowers the 3-D peaking factors.

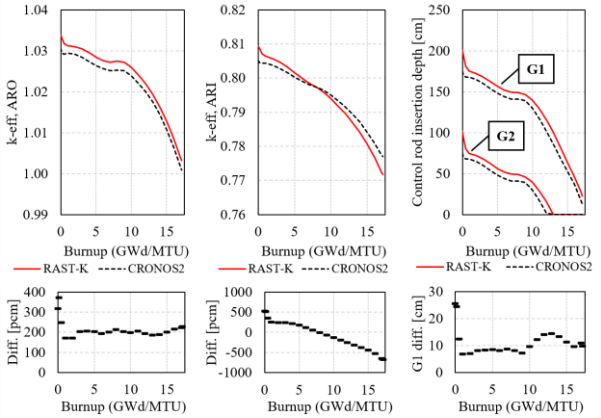


Fig. 4. Core k_{eff} in the ARO (left) and ARI (center) states, and insertion depth of the G1 and G2 banks (right).

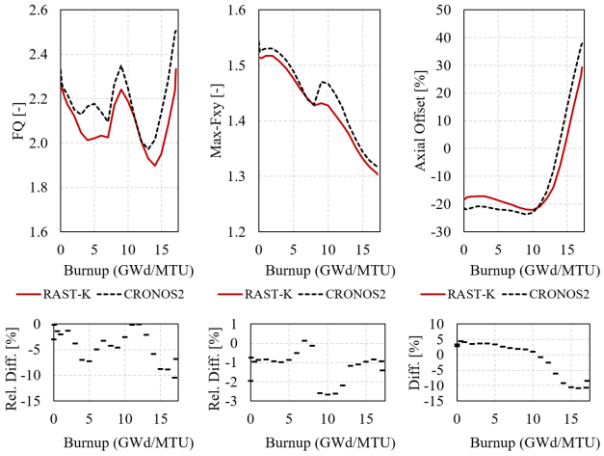


Fig. 5. Evolution of F_q, F_{xy} and AO during the equilibrium cycle.

Fig. 6 compares the radial power and burnup distributions at BOC and EOC. The deviation pattern at BOC follows the control bank arrangement shown in Fig. 2. The largest local power deviation of -8.04% appears at the G2 position. The G1 positions show deviations of -5.34% and -3.32%. The peripheral positions without an inserted bank show positive deviations of up to 4.55%. The spatial correlation confirms that the deeper insertion in RAST-K suppresses the power in the rodded region and shifts it toward the periphery. The deviations are reduced to within 1.8% at EOC, where the banks are almost fully withdrawn. The burnup distribution at EOC exceeds the reference at every position, since the RAST-K cycle is 2.35% longer. The deviation ranges from 1.30% to 4.74% around the offset. The minimum appears at the G2 position and the maximum at the periphery, which reflects the power redistribution accumulated over the cycle.

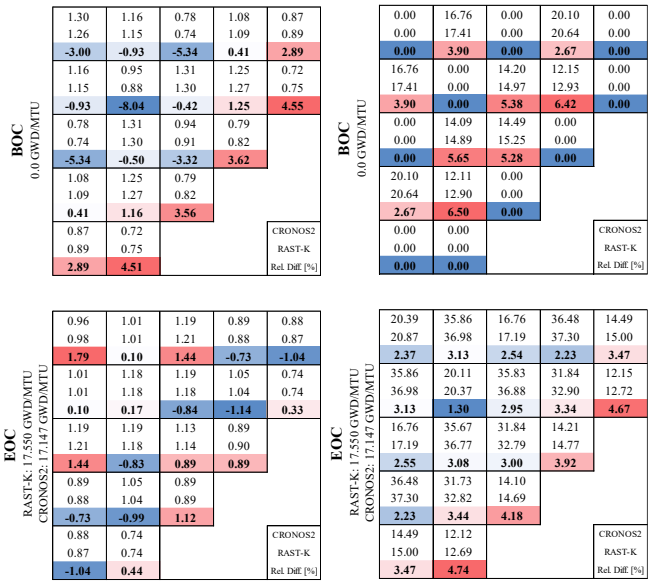


Fig. 6. Radial power (left) and burnup (right) distribution.

4. Conclusions

The PRATIC Soluble-Boron-Free SMR benchmark was analyzed with the STREAM/RAST-K code system, and the results were compared against the CEA reference solutions with the APOLLO2.8-5/CRONOS2 code system.

At the assembly level, the k_∞ evolution of the five fuel types agreed with the reference within about 600 pcm over the entire depletion range, and the RMS difference did not exceed 283 pcm for any type.

At the core level, the equilibrium cycle search converged to a cycle length of 17.550 GWd/MTU, which is 2.35% longer than the reference. The higher excess reactivity predicted by RAST-K led to a deeper control rod insertion of about 26 cm at BOC, and the resulting suppression of the central power produced lower peaking factors than the reference over most of the cycle. The radial power and burnup distributions reproduced the reference patterns, and the largest local deviation appeared at BOC and decreased toward EOC as the control banks were withdrawn. Overall, STREAM/RAST-K reproduced the neutronic behavior of the PRATIC equilibrium cycle consistently, and the observed differences are comparable to those reported between other deterministic code systems for this benchmark [2].

The assembly comparison was performed with the same library, and the nuclear data effect was quantified separately from the two APOLLO2 solutions. At the core level the reference is available only with JEFF-3.1.1. A JEFF-3.1.1 library is not currently available for STREAM, so the present calculations could not be repeated with the reference library. A Monte Carlo

analysis of the same benchmark with both libraries is planned. The calculation will provide a reference solution for the two-step scheme and will quantify the library contribution at the core level directly.

REFERENCES

[1] R. Vuiart et al., "PRATIC: A soluble-boron-free, pressurized water cooled, SMR core benchmark", *EPJ Nuclear Sci. Technol*. **10**, *25* (2024).

[2] R. Vuiart et al., "Modeling the equilibrium cycle of the PRATIC SMR core benchmark using the CMS5 code system", *Proc. of ICAPP*, Antibes, Juan les Pins, France, September 17-19 (2025).

[3] J.-B. Schuler et al., "SERPENT2 and CMS5 Depletion Modeling of the PRATIC SMR Startup Core Benchmark", *SSRN Preprint 7155066* (2025).

[4] A. Eustache et al., "Development of the PRATIC-b Soluble-Boron-Controlled core and Benchmarking Using APOLLO2-CRONOS2, CMS5 and APOLLO3", *Proc. of PHYSOR2026*, Torino, Italy, April 19-23 (2026).

[5] S. Choi et al., "Resonance treatment using pin-based pointwise energy slowing down method", *Journal of Computational Physics* **330**, *134* (2017).

[6] J. Choe et al., "Verification and Validation of STREAM/RAST-K for PWR analysis", *Nuclear Engineering and Technology, Vol. **51**, p.356-368,* (2019).